

Preparation of Nitrogen-doped TiO₂ Nanoparticle Catalyst and Its Catalytic Activity under Visible Light*

YU Huang(於煌), ZHENG Xuxu(郑旭煦)**, YIN Zhongyi(殷钟意), TAO Feng(陶丰), FANG Beibei(房蓓蓓) and HOU Keshan(侯苛山)

College of Environment and Bioengineering, Chongqing Technology and Business University, Chongqing 400067, China

Abstract N-doped TiO₂ nanoparticle photocatalysts were prepared through a sol-gel procedure using NH₄Cl as the nitrogen source and followed by calcination at certain temperature. Systematic studies for the preparation parameters and their impact on the structure and photocatalytic activity under ultraviolet (UV) and visible light irradiation were carried out. Multiple techniques (XRD, TEM, DRIF, DSC, and XPS) were commanded to characterize the crystal structures and chemical binding of N-doped TiO₂. Its photocatalytic activity was examined by the degradation of organic compounds. The catalytic activity of the prepared N-doped TiO₂ nanoparticles under visible light ($\lambda > 400\text{nm}$) irradiation is evidenced by the decomposition of 4-chlorophenol, showing that nitrogen atoms in the N-doped TiO₂ nanoparticle catalyst are responsible for the visible light catalytic activity. The N-doped TiO₂ nanoparticle catalyst prepared with this modified route exhibits higher catalytic activity under UV irradiation in contrast to TiO₂ without N-doping. It is suggested that the doped nitrogen here is located at the interstitial site of TiO₂ lattice.

Keywords photocatalysis, TiO₂, visible light, nitrogen-doping, preparation

1 INTRODUCTION

Since the report of photoelectrochemical decomposition of water on titanium dioxide electrode in 1972[1], the chemical stability, nontoxicity, and high photocatalytic reactivity of TiO₂ has attracted tremendous attention. However, TiO₂ without doping is active only by irradiating with ultraviolet light because of its large band gap of 3.2eV (anatase). This band gap limits the use of the wide energy window of sun light because solar energy is the most important alternative energy source in the future[2]. To shift the optical response of catalytically active TiO₂ from ultraviolet (UV) to visible light, different studies have been carried out to modify TiO₂ to tune the band gap of TiO₂ for an absorption of visible light. Among these studies, nitrogen doping[3—6] is one of the most important methods for a promising application.

The reported nitrogen doping for TiO₂ mainly includes (1) sputtering TiO₂ target for several hours in an N₂/Ar gas mixture and then annealing in N₂ gas[7,8], (2) treating anatase TiO₂ powder in an NH₃/Ar atmosphere[7,9—11], and (3) a hydrolytic process using titanium alkoxide or chloride solution and an ammonia solution[12,13]. The first method needs expensive experimental facilities. The second and third routes are not environmentally friendly because of their use of ammonia. In principle, the combined sol-gel and calcination is an economic and reasonable method for the preparation of TiO₂ catalyst. However, there is an absence of a systematic investigation for the influence of preparation parameters on the formed crystal structures and the photocatalytic activity in this preparation strategy. Thus, here we used a modified sol-gel route for the preparation of

N-doped TiO₂ and a relatively environmentally friendly NH₄Cl as nitrogen source. Multiple analytic techniques were used to monitor the intermediates and products at different stages of the preparation route. Preparation parameters including acidity of the solution of precursor, calcination temperature, and their impact on crystallization of TiO₂ xerogel mixed with NH₄Cl and photocatalytic activity of the N-doped TiO₂ were systematically studied. The dependence of the formed crystal structure and the photocatalytic activity on calcination temperature was revealed. The importance of pH of the precursor solution for the photocatalytic activity of the formed catalysts was demonstrated. An optimized preparation route was obtained, by which the prepared N-doped TiO₂ nanoparticle catalyst has obvious catalytic activity under visible light irradiation. Our studies suggest that the nitrogen is incorporated into interstitial sites which contribute to the appearance of catalytic activity under visible light irradiation and the obvious enhancement of activity under UV irradiation in contrast to TiO₂ without N-doping.

2 EXPERIMENTAL

2.1 Synthesis of N-doped TiO₂ catalyst

Tetra-butyl titanate [Ti(OBu)₄, 5ml, 97%] was dissolved in 95ml anhydrous alcohol. Into the solution of Ti(OBu)₄ was added 5ml NH₄Cl (1mol·L⁻¹), dropwise, under stirring to carry out hydrolysis. The pH of the solution with NH₄Cl was controlled at a certain value. The gel was left for aging for one day at room temperature and subsequently dried at 70°C for several hours. Finally, the dried material was calcined at dif-

Received 2006-12-21, accepted 2007-06-11.

* Supported by the Science and Technology Research Program of Chongqing Education Commission (KJ050702), and the Natural Science Foundation Project of Chongqing Science and Technology Commission (No.2007BB7208).

** To whom correspondence should be addressed. E-mail: zxx_chem@hotmail.com

ferent temperature to obtain N-doped TiO₂ nanoparticle catalyst with different doping level of nitrogen.

2.2 Analytical methods

The X-ray powder diffraction (XRD) patterns were recorded on a Shimadzu LabX-600 diffractometer with Cu K_α radiation ($\lambda=0.1548\text{nm}$). The size of the prepared nanoparticles was determined using the Scherrer formula $L=K\lambda/(\beta\cos\theta)$, where K is a constant of 0.89, λ is the wavelength characteristic of the Cu K_α radiation, β is the full width at half maximum (in radians), and θ is the angle at which the (100) peak appears. The mass percent of anatase in the product was obtained from the equation [14]: $X_A=[1+1.26(I_R/I_A)]^{-1}$, where X_A is the mass fraction of anatase in the mixture, I_A and I_R were obtained from the peak areas of anatase (101) and rutile (110) diffraction peaks, respectively. The morphology and sizes of the particles were examined using transmission electron microscopy (TEM) (Philips TECNAI 10 at 100kV). The diffuse reflectance infrared Fourier transform (DRIFT) spectra of the samples were measured on a Shimadzu IRPrestige-21 spectrometer. Thermal analysis was carried out on a differential scanning calorimeter (DSC) (Shimadzu, DSC-60) in N₂ atmosphere of 60ml·min⁻¹ at a heating rate of 10°C·min⁻¹ from room temperature to 600°C. N1s core level of the N-doped TiO₂ was measured with VG MultiLab 2000 system using Mg K_α (1253.6eV) radiation as X-ray source. The binding energies were calibrated with standard method.

2.3 Measurement of photocatalytic activity

The photocatalytic activity of the N-doped TiO₂ nanoparticle catalysts was characterized by photodegradation of methylene blue (MB) under UV light irradiation and 4-chlorophenol under visible light irradiation. For an examination of the catalytic activity under UV light irradiation, 100ml 20mg·L⁻¹ MB aqueous solution with 0.05g catalyst was loaded in a glass container and mixed using a magnetic stirrer. The solution containing N-doped TiO₂ catalyst was left for 30min in a dark box and the solution was irradiated with a 30-W mercury lamp. In every 20min, 10ml solution was taken out and filtered through a 0.20mm membrane filter. To determine the catalytic activity of N-doped TiO₂ under visible light irradiation, 4-chlorophenol (13mg·L⁻¹) was used as a model compound. The visible 500-W xenon lamp was used as a visible light source upon blacking UV light by a 400nm glass filter. The concentrations of MB and 4-chlorophenol taken from the solution in a sequence were determined by UV absorbance spectrometer (751GD, Shanghai Analysis Apparatus Factory).

3 RESULTS AND DISCUSSION

3.1 Catalyst characterization

Figure 1 depicts the XRD patterns of the samples calcined at different temperatures. The N-doped samples exhibit an almost amorphous structure at 300°C, complete anatases structure at 400°C and 500°C, and mixed structures of both anatase and rutile phases at

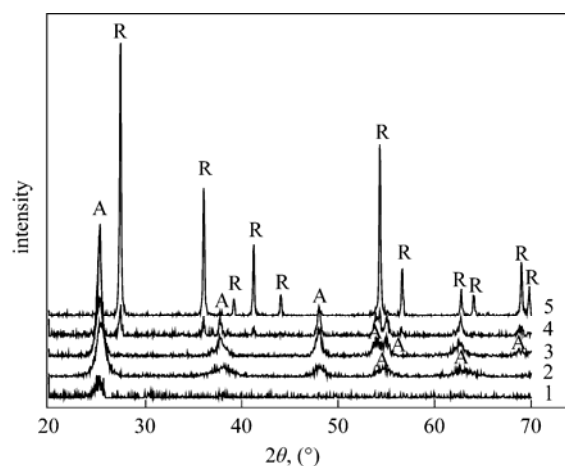


Figure 1 XRD patterns of N-doped TiO₂ calcined at different temperatures (A: anatase, R: rutile) temperature, °C: 1—300; 2—400; 3—500; 4—600; 5—700

600°C and 700°C. The temperature evolution shown in Fig.1 shows that the peak intensity of anatase increases and the width of the (101) diffraction peak of anatase phase ($2\theta=25.28^\circ$) becomes narrower with the increase of calcination temperature (from 400°C to 500°C). This suggests that the particle size of N-doped TiO₂ nanoparticles increases from 400°C to 500°C. Table 1 summarizes the phase structures and particle sizes of the prepared N-doped TiO₂ in the temperature range of 400—700°C. Clearly, calcination temperature plays a significant role in the formed crystal structure and particle size. Higher temperature favors the growth of rutile structure and produces N-doped TiO₂ nanoparticles with larger particle size. Thus, a fine control of calcination temperature is crucial for obtaining a pure phase of N-doped TiO₂.

Table 1 Influence of temperature on particle size and crystal phase of N-doped TiO₂

Temperature, °C	Particle size, nm	Crystal phase
300	—	—
400	8.2	100%A
500	14.1	100%A
600	26.9(A), 33.3(R)	81.4%(A), 18.6%(R)
700	40.4(A), 66.4(R)	6.7%(A), 93.3%(R)

The particle sizes of the powders calcined at 400°C, 500°C, 600°C, 700°C examined with TEM are 10—20nm, 15—30nm, 20—40nm, and 20—90nm, respectively. The obvious increase of particle size from 600°C to 700°C possibly results from aggregation at high temperature. The particle sizes examined with TEM are consistent with those calculated from XRD patterns listed in Table 1. Fig.2 is TEM images of the N-doped TiO₂ powders calcined at 500°C, 600°C and 700°C.

To understand the evolution of nitrogen source in the preparation route, DRIFT was used to obtain the

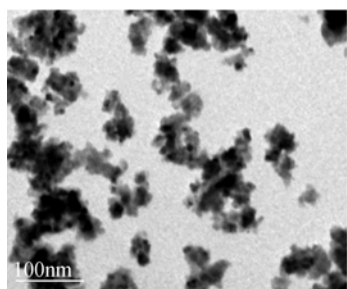
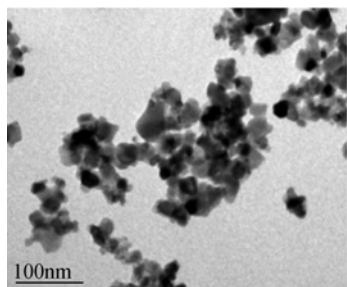
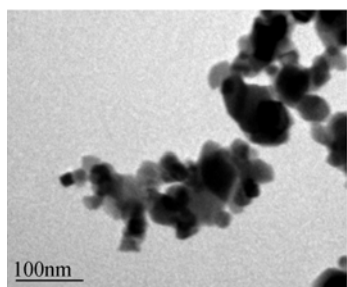
(a) $T=500^{\circ}\text{C}$ (b) $T=600^{\circ}\text{C}$ (c) $T=700^{\circ}\text{C}$

Figure 2 TEM images of the N-doped TiO_2 nanocomposites calcined at 500°C , 600°C and 700°C

vibrational signature of the intermediate before calcination. Fig.3 presents the DRIFT spectra of TiO_2 without calcination and TiO_2 xerogel mixed with NH_4Cl without calcination. The wide band at $3100\text{--}3500\text{cm}^{-1}$ which appears in the spectrum of TiO_2 is because of the adsorbed water and the formed hydroxyl group. Compared with TiO_2 without N-doping, two new bands at 3132cm^{-1} and 1402cm^{-1} , attributed

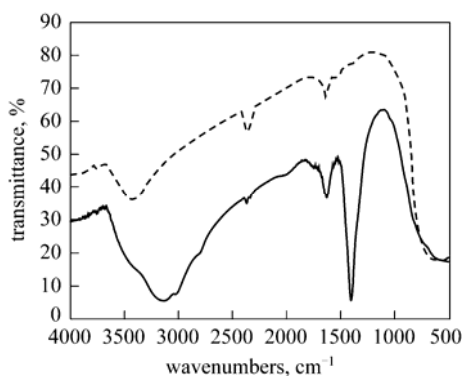


Figure 3 DRIFT spectra of undoped- TiO_2 and N-doped TiO_2

to NH_4^+ [15], appear in the spectrum of TiO_2 xerogel mixed with NH_4Cl . It shows that the NH_4^+ species are absorbed on the surface of TiO_2 before calcination and act as the nitrogen source for incorporation during calcinations [16]. The band at $450\text{--}470\text{cm}^{-1}$ appeared in the spectra of TiO_2 and TiO_2 xerogel mixed with NH_4Cl can be assigned to Ti—O stretching mode.

Figure 4 shows DSC curve of TiO_2 xerogel mixed with NH_4Cl without calcination. A big endothermic peak at about 102°C was caused by desorption of the physisorbed water and alcohol. The relatively small endothermic peak at 303°C possibly results from the desorption of unhydrolyzed $\text{Ti}(\text{O}i\text{Bu})_2$ remained in the N-doped TiO_2 xerogel. The DSC curve also shows a significant exothermic peak at about 408°C , which is possibly because of the phase transformation from amorphous to anatase. There is no detectable exothermic peak at a temperature higher than 460°C , showing that TiO_2 gel prepared from sol-gel route containing-N has almost been crystallized into anatase upon calcination. Thus, 408°C is the crystallization temperature of TiO_2 gel containing-N from amorphous to anatase. This result is consistent with the Ref.[12] and our XRD analysis described earlier.

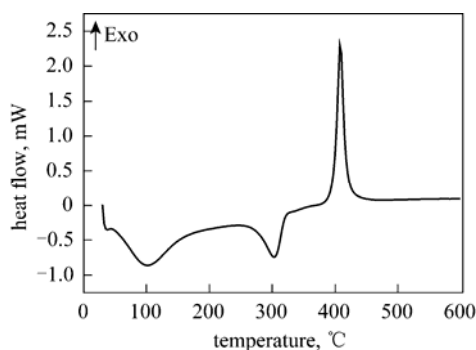


Figure 4 DSC curve of N-doped TiO_2

Figure 5 illustrates the light absorption properties of TiO_2 calcined at 500°C and N-doped TiO_2 calcined at 500°C . The visible absorption spectra show that the N-doped TiO_2 is a photocatalyst with the capability of photocatalysis under visible light irradiation. The band gap of the samples was determined by the equation [17].

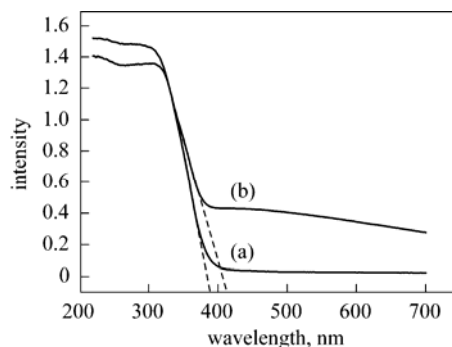


Figure 5 UV-Vis absorption spectra of TiO_2 (a) and N-doped TiO_2 (b) calcined at 500°C

$$E_g = 1239.8 / \lambda$$

where E_g is the band gap (eV) and λ (nm) is the wavelength of the absorption edge in the spectrum. Compared with TiO₂ without N-doping, the band gap was changed from 3.20eV to 3.00eV of N-doped TiO₂. This change demonstrates a strategy for shaping photocatalysis by an atomic-level doping for nanocatalyst. In addition, the absorption spectra of the N-doped TiO₂ samples also showed a stronger absorption than TiO₂ without N-doping under UV irradiation, indicating that N-doping could be a promising approach for increasing the catalytic activity. The increase of the catalytic activity upon N-doping is different from the previous study[7,18]. This difference could result from our different preparation route and nitrogen source. Further study and mechanistic understanding is under investigation.

Figure 6(b) depicts the photoemission feature of the N1s core level of the prepared N-doped TiO₂ nanoparticle catalyst. The TiO₂ without N-doping is taken as a reference here [Fig.6(a)]. No observable N1s photoemission feature for TiO₂ calcined at 500°C, as shown in Fig.6(a), shows that molecular nitrogen in air cannot be incorporated into TiO₂ lattice under calcination at 500°C. This is so though N₂ is a nitrogen source for the growth of TiO_{2-x}N_x film by sputtering TiO₂ target in N₂/Ar mixture gas and annealed to high temperature in N₂ gas[7,8]. However, the observation of an obvious peak at about 398.6eV as seen in Fig.6(b) suggests that nitrogen of NH₄⁺ is incorporated into TiO₂ lattice upon calcination. Notably, a peak of N1s core level at 396.7eV was reported for N-doped TiO₂ by other group using different preparation route[19]. The doped nitrogen was understood as a substitute for oxygen atom of TiO₂ lattice. Compared with the low-binding energy at 396.7eV resulting from electron transfer from Ti with low electronegativity to N atom, the doped nitrogen of our samples has a higher binding energy at 398.6eV. This difference suggests that the doped nitrogen in TiO₂ prepared with our route has different structural geometry and chemical binding in TiO₂ lattice. It possibly rationalizes the different catalytic activity under UV light irradiation described earlier in contrast to the previous studies[7,18]. It is suggested that the doped nitrogen atoms in our sample are possibly located at

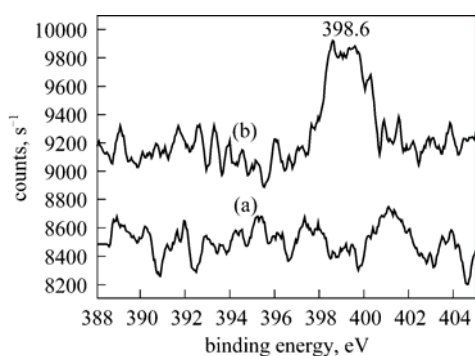


Figure 6 N1s XPS spectra of TiO₂ (a) and N-doped TiO₂ (b) calcined at 500°C

interstitial sites, which has a weak binding with Ti atoms. The N1s binding energy seen in Fig.6(b) is consistent with that of NH_x-containing compound[20], indicating that NH₄⁺ does not completely decompose into nitrogen atom during calcination.

3.2 Influential factors of photocatalytic activity

3.2.1 Influence of calcination temperature on photocatalytic activity

Figure 7 presents the photocatalytic activity of different N-doped TiO₂ samples under UV irradiation as a function of calcination temperature. MB is used as a probe for determining the catalytic activity under UV irradiation. The photocatalytic activity of the samples increases with the increase of calcination temperature from 300°C to 500°C. At 500°C it reaches the maxima because of a complete crystallization of anatase at this temperature. However, the catalytic activity of N-doped TiO₂ decreases obviously with the increase of calcination temperature from 500°C to 700°C. This is consistent with the fact that anatase is more photocatalytically active than rutile phase, and more anatase was converted into rutile phase at a higher calcination temperature between 500°C and 700°C (Fig.1 and Table 1). The importance of calcination temperature is demonstrated here.

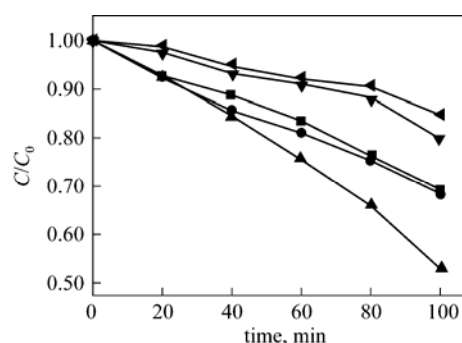


Figure 7 Photoactivity of N-doped TiO₂ calcined at different temperatures under UV light temperature, °C: ■ 300; ● 400; ▲ 500; ▼ 600; ◀ 700

3.2.2 Influence of pH of the solution of precursor on photocatalytic activity

Figure 8 shows that the photocatalytic activity of N-doped TiO₂ is prepared in a solution of precursor with different acidity (pH=2–5) and then calcined at 500°C. The photocatalytic activity of N-doped TiO₂ nanoparticle catalyst increases when the value of pH decreases from 5 to 3, at which it reaches a maxima. The possible reason is that the increase of H⁺ concentration along with the decrease of pH restrains hydrolyzation of Ti(OBu)₄ and thereby results in the decrease of the crystal size of the prepared N-doped TiO₂ nanoparticles. However, pH cannot be too low. Too low pH such as 2 would result in a phase transformation from anatase to rutile[21], supported by the low photocatalytic activity of the samples prepared at pH=2.

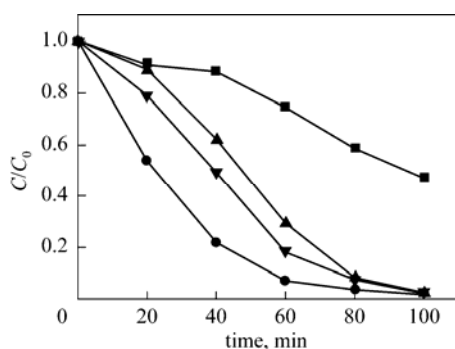


Figure 8 Photoactivity of N-doped TiO₂ prepared at different pH under UV light
pH: ■ 2; ● 3; ▼ 4; ▲ 5

3.3 Visible light activity

The aforementioned systematic investigations show that the N-doped TiO₂ exhibits the largest catalytic activity under UV light irradiation at the calcination temperature of 500 °C and pH=3. To explore the visible light activity of N-doped TiO₂ nanoparticle catalyst prepared at this condition, 500-W xenon lamp with a 400nm cut-off filter was used as a visible light source. In order to avoid the dye-sensitized effect of MB, 4-chlorophenol was used as a new probe. The catalytic activity of undoped-TiO₂ and N-doped TiO₂ nanoparticles was examined (Fig.9). Obviously, N-doped TiO₂ can degrade 4-chlorophenol under visible light ($\lambda > 400\text{nm}$) irradiation with a 63.5 % conversion upon 6h, whose visible light activity is little better than the reported activity[22]. TiO₂ without any doping could not degrade 4-chlorophenol under the same condition. Thus, the TiO₂ without N-doping is not catalytically active under visible light irradiation for this reaction. As implied by XPS data in Fig.6, the doped nitrogen is possibly located at interstitial sites, it may give rise to a midgap (N-2p) level slightly above the top of the (O-2p) valence band. The electron is transferred from the midgap band to conduction band of TiO₂ and thereby induces catalytic activity under visible light irradiation[4,9].

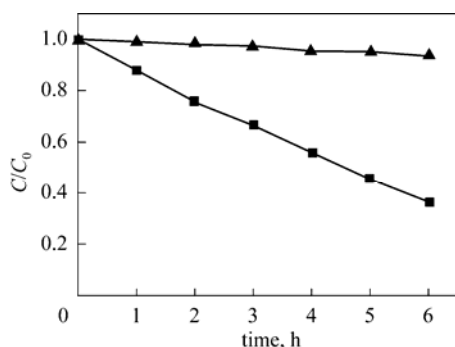


Figure 9 Photoactivity of TiO₂ and N-doped TiO₂ under visible light
■ N-doped TiO₂; ▲ TiO₂

4 CONCLUSIONS

N-doped TiO₂ nanoparticle catalysts exhibiting

photocatalytic activity under UV and visible light irradiation were successfully prepared by a modified sol-gel procedure using NH₄Cl as nitrogen source followed by calcination at a certain temperature. Our investigations revealed that the acidity (pH value) of the solution of precursor and the subsequent calcination temperature have a significant impact on the crystallization of xerogel and the particle size of the formed N-doped TiO₂ nanoparticle catalyst, and the photocatalytic activity. Systematical studies showed that N-doped TiO₂ nanoparticle catalyst prepared at a solution with pH=3 and calcination temperature of 500 °C has the largest photocatalytic activity. It is suggested that the NH₄⁺ species were absorbed on the surface of TiO₂ gel at low temperature and subsequently incorporated into the TiO₂ lattice during calcination at high temperature. The N-doped TiO₂ exhibits higher activity than TiO₂ without N-doping under UV irradiation. N-doped TiO₂ nanoparticle catalyst has obvious visible light activity, evidenced by the degradation of 4-chlorophenol under visible light ($\lambda > 400\text{nm}$) irradiation. However, the catalytic activity under visible light irradiation is absent for TiO₂ without N-doping. Further studies on the geometric structure and chemical binding of the doped nitrogen in the TiO₂ lattice are in progress.

REFERENCES

- Fujishima, A., Honda, K., "Electrochemical photolysis of water at a semiconductor electrode", *Nature*, **238**, 37—38(1972).
- Gole, J.L., Stout, J.D., Burda, C., Lou, Y., Chen, X., "Highly efficient formation of visible light tunable TiO_{2-x}N_x photocatalysts and their transformation at the nanoscale", *J. Phys. Chem. B*, **108**(4), 1230—1240(2004).
- Wang, Z., Cai, W., Hong, X., Zhao, X., Xu, F., Cai, C., "Photocatalytic degradation of phenol in aqueous nitrogen-doped TiO₂ suspensions with various light sources", *App. Catal. B*, **57**(3), 223—231(2005).
- Nakamura, R., Tanaka, T., Nakato, Y., "Mechanism for visible light responses in anodic photocurrents at N-doped TiO₂ film electrodes", *J. Phys. Chem. B*, **108**(30), 10617—10620(2004).
- Jang, J.S., Kim, H.G., Ji, S.M., Bae, S.W., Jung, J.H., Shon, B.H., Lee, J.S., "Formation of crystalline TiO_{2-x}N_x and its photocatalytic activity", *J. Solid State Chem.*, **179**(4), 1067—1075(2006).
- Yin, S., Ihara, K., Komatsu, M., Zhang, Q., Saito, F., Kyotani, T., Sato, T., "Low temperature synthesis of TiO_{2-x}N_y powders and films with visible light responsive photocatalytic activity", *Solid State Commun.*, **137**(3), 132—137(2006).
- Asahi, R., Morikawa, T., Ohwaki, T., Aoki, K., Taga, Y., "Visible-light photocatalysis in nitrogen-doped titanium oxides", *Science*, **293**(5528), 269—271(2001).
- Wong, M.S., Chou, H.P., Yang, T.S., "Reactively sputtered N-doped titanium oxide films as visible-light photocatalyst", *Thin Solid Films*, **494**(1/2), 244—249(2006).
- Irie, H., Watanabe, Y., Hashimoto, K., "Nitrogen-concentration dependence on photocatalytic activity of TiO_{2-x}N_x powders", *J. Phys. Chem. B*, **107**(23), 5483—5486(2003).
- Kosowska, B., Mozia, S., Morawski, A.W., Grzmil, B., Janus, M., Kalucki, K., "The preparation of TiO₂-nitrogen doped by calcination of TiO₂ middle dot xH₂O under ammonia atmosphere for visible light photocatalysis", *Sol. Energ. Mat. Sol. C.*, **88**(3), 269—280(2005).

- 11 Mozia, S., Tomaszewska, M., Kosowska, B., Grzmil, B., Morawski, A.W., Kalucki, K., "Decomposition of non-ionic surfactant on a nitrogen-doped photocatalyst under visible-light irradiation", *App. Catal. B*, **55**(3), 195—200(2005).
- 12 Sato, S., Nakamura, R., Abe, S., "Visible-light sensitization of TiO₂ photocatalysts by wet-method N doping", *Appl. Catal. A*, **284**(1/2), 131—137(2005).
- 13 Liu, Y., Chen, X., Li, J., Burda, C., "Photocatalytic degradation of azo dyes by nitrogen-doped TiO₂ nanocatalysts", *Chemosphere*, **61**(1), 11—18(2005).
- 14 Spurr, R.A., Myers, H., "Quantitative analysis of anatase-rutile mixtures with an X-ray diffractometer", *Anal. Chem.*, **29**(5), 760—762(1957).
- 15 Ihara, T., Miyoshi, M., Iriyama, Y., Matsumoto, O., Sugihara, S., "Visible-light-active titanium oxide photocatalyst realized by an oxygen-deficient structure and by nitrogen doping", *App. Catal. B*, **42**(4), 403—409(2003).
- 16 Kuroda, Y., Mori, T., Yagi, K., Makihata, N., Kawahara, Y., Nagao, M., Kittaka, S., "Preparation of visible-light-responsive TiO_{2-x}N_x photocatalyst by a sol-gel method: Analysis of the active center on TiO₂ that reacts with NH₃", *Langmuir*, **21**(17), 8026—8034(2005).
- 17 O'Regan, B., Gratzel, M., "A low-cost, high-efficiency solar cell based on dye-sensitized colloidal TiO₂ films", *Nature*, **353**(6346), 737—740(1991).
- 18 Wang, Z.P., Cai, W.M., Hong, X.T., Zhao, X.L., Xu, F., Cai, C.G., "Photocatalytic degradation of phenol in aqueous nitrogen-doped TiO₂ suspensions with various light sources", *Appl. Catal. B*, **57**(3), 223—231(2005).
- 19 Saha, N.C., Tompkins, H.G., "Titanium nitride oxidation chemistry: An X-ray photoelectron spectroscopy study", *J. Appl. Phys.*, **72**(7), 3072—3079(1992).
- 20 Souto, S., Alvarez, F., "The role of hydrogen in nitrogen-containing diamondlike films studied by photoelectron spectroscopy", *Appl. Phys. Lett.*, **70**(12), 1539—1541(1997).
- 21 Chen, X., Gu, G., "Study on synthesis of nanometer TiO₂ crystal from organic compound in liquid phase at normal pressure and low temperature", *Chin. J. Inorg. Chem.*, **18**(7), 749—752(2002).
- 22 Sakthivel, S., Kisch H., "Photocatalytic and photoelectrochemical properties of nitrogen-doped titanium dioxide", *Chemphyschem*, **4**(5), 487—490(2003).